CAD-Based Calculation of Cutting Force Components in Gear Hobbing

Tapoglou Nikolaos
Ph.D. Candidate
e-mail: ntapoglou@isc.tuc.gr

Antoniadis Aristomenis[1]
Associate Professor
e-mail: antoniadis@dpem.tuc.gr

Department of Production Engineering and Management,
Technical University of Crete,
University Campus, Kounoupidiana,
Chania, Crete 73100, Greece

Gear hobbing is a common method of manufacturing high precision involute gears. The thorough knowledge of the developed cutting forces and the wear of the cutting tool are of great importance in order to produce helical and spur gears as they influence the cost of the manufacturing process and the quality of the produced gear. A novel simulation code called HOB3D was created in accordance with the above. This code can simulate the complex movements involved in gear hobbing with the best available accuracy, which is achieved by embedding the developed algorithm in a commercial computer aided design (CAD) environment. The simulation code calculates and exports the total cutting forces as well as the cutting forces in every cutting edge involved in the cutting process.
[DOI: 10.1115/1.4006553]

Keywords: gear manufacturing, gear hobbing, cutting forces

1 Introduction

Every high performance gear transmission module is composed of involute gears. External involute gears can be manufactured with a series of methods, of which gear hobbing is the most widely applied. The prediction of the quality of the produced gear and the determination of the cutting forces involved are of great importance. A novel simulation code was developed aiming at the simulation of the gear hobbing process. This code, called HOB3D, can simulate the cutting process in a commercial CAD environment, thus producing results determined with the optimal precision.

2 State of the Art

Gear hobbing process, as opposed to turning and milling, is a sophisticated metal removal technology owing to the complexity of hobbing cutters geometry and the advanced kinematics of the process. The process is based on three relative motions between the workpiece and the hob tool. Due to the generating rolling principle, complex tool geometry, different chip flow mechanisms, and complex kinematics, the simulation of gear hobbing process is quite difficult. A first approach toward the simulation of gear hobbing was made in the 1970s with the FRS code [1,2]. This code could simulate the process with the aid of numerical approximation and the results produced include chip dimensions and cutting force components.

In the field of force prediction, Gutman calculated the cutting forces using cross-sections of the chip produced by the FRS model [3]. His model was verified with sets of experiments he conducted. An area of great interest is the wear progress determination through experiments. Tondorf conducted experiments in order to observe the wear of hobs and to optimize cutting conditions in order to avoid built up edge [4], whereas Venohr studied the use of carbide tools in gear hobbing, conducting experiments in order to study their wear progress [5]. Tool stresses in the cutting edge of the tool were investigated by Antoniadis using the nondeformed chip geometries produced by the FRS model [6]. Based on the previous work, Antoniadis et al. proposed a model for wear prediction with the aid of a finite elements method (FEM) model [7]. This model's validity was verified with experiments carried out by Antoniadis et al. [8]. Bouzakis et al. also developed a wear prediction model using the nondeformed chip geometries optimizing in the same time the number of tangential shifts of the hob in order to produce a uniform wear along the hob [9]. The numerical approximations presented above make use of simplifications and projections in their model and produce less accurate results. Lately, FEM and CAD software packages can support chip removal calculation and analysis. In this area, researchers have developed CAD and FEM models that predict the deformed chip geometry as well as the mechanical stresses on the cutting tool [10–12]. The work presented above emphasizes more on the chip geometry, whereas the work of other researchers is more focused on the 3D gap. In their research, Michalski and Skoczylas used a CAD environment to model the flanks of hobbed gears [13]. Focusing on the realistic and accurate simulation of the gear hobbing process, a 3D approach for the simulation of manufacturing spur and helical gears is presented in this research paper.

3 Gear Hobbing and HOB3D Simulation Process

The kinematics of gear hobbing consists of three relative movements between the workgear and the hob. These movements have to be synchronized in order to produce the required gear. The first movement, which is marked as 1 in the left picture of Fig. 1, is the rotation of the hob around its own axis. The second is the axial feed of the hob, marked as 2 and the last movement is the rotation of the workgear around its axis, marked as 3.

The geometry of a gear can be defined based on six parameters: module (m), number of teeth (z_2), outside diameter (d_g), helix angle (h_a), gear width, and pressure angle (a_n). In order to fully define the kinematic chain of gear hobbing, a series of other parameters must be established. These parameters are hob diameter (d_h), number of columns (n_i), number of hob origins (z_1), depth of cut (t), axial feed (f_a), and cutting speed (v). Finally, there are more parameters such as the helix angle of the hob (γ) and the axial pitch (ε), which already exist or can be calculated. The setting angle of the hob relative to the workgear is of great importance in the process and is determined by the parameters mentioned above, being equal to the difference between the helix angle of the workgear and the helix angle of the hob. The direction of the axial feed (f_a) defines two different hobbing strategies: the climb hobbing (CL) and the up-cut hobbing (UC). In case of helical gears, two additional variations exist, arising from the

[1]Corresponding author.

Contributed by the Manufacturing Engineering Division of ASME for publication in the JOURNAL OF MANUFACTURING SCIENCE AND ENGINEERING. Manuscript received June 4, 2011; final manuscript received March 2, 2012; published online May 7, 2012. Assoc. Editor: Tony Schmitz.

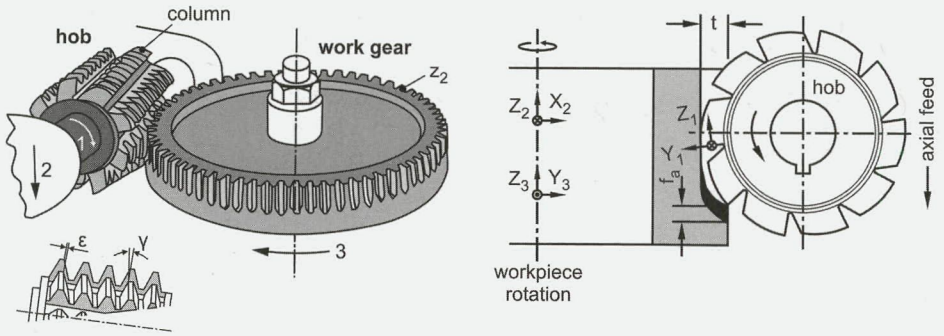

Fig. 1 Basic kinematics of gear hobbing

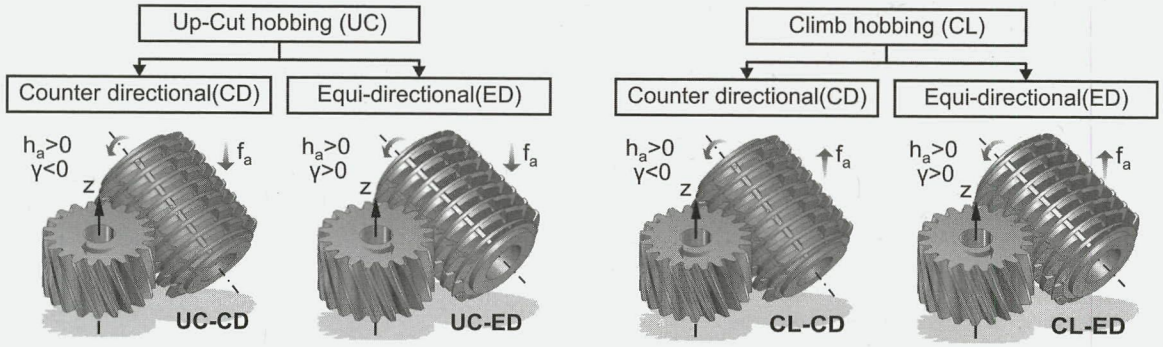

Fig. 2 The four possible kinematics of gear hobbing considering the direction of the axial feed and the applied gearing

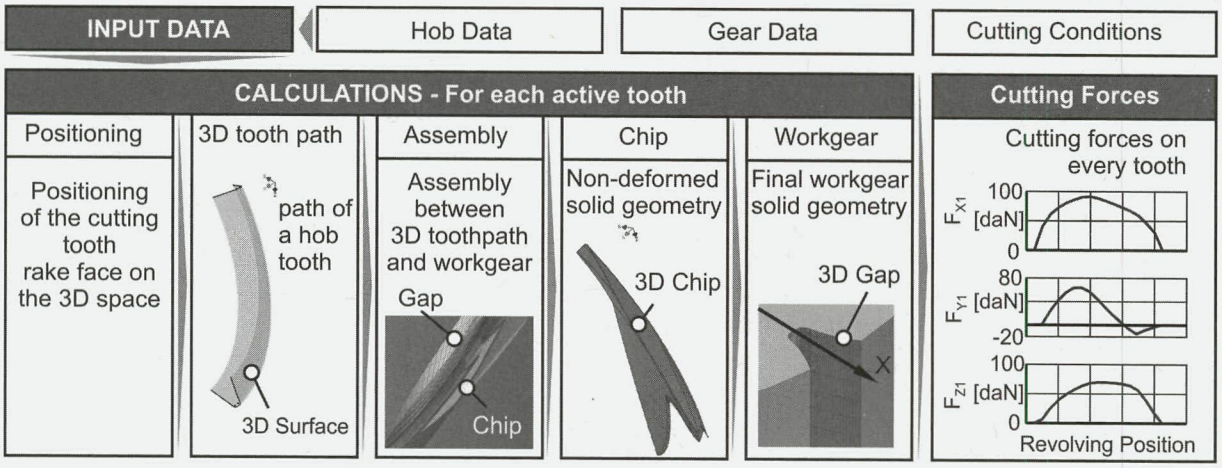

Fig. 3 HOB3D flowchart

comparison between the tool helix angle (γ) and the helix of the gear (h_a). If the direction of the gear helix angle is identical to the hob helix angle, the type of the process is defined as equidirectional hobbing; if not, as counterdirectional hobbing. The four different hobbing strategies are illustrated in Fig. 2.

In order to simulate the process of gear hobbing, new software has been developed. The proposed simulation model has been embedded in a commercial CAD program, thus taking advantage of its accuracy, also resulting in more accurate calculations. The model is capable of calculating the nondeformed chip geometry, the 3D gap geometry, and the cutting forces involved in the production of spur as well as in helical involute gears. The new simulation code called HOB3D uses three coordinate systems in order to calculate the required results. The first (1) is positioned on the examined cutting edge and has the X axis parallel to the hob's axis, the Y axis perpendicular to X axis and rests on the rake face, finally Z axis perpendicular to the prior two. Coordinate systems (2) and (3) have axis Z running through the workgear's axis. In coordinate system (2), X axis is always rotating toward the direction of the gap center while the axes of coordinate system (3) are fixed.

The simulation process of HOB3D is initialized after the input of valid data. Due to the fact that the gear is axisymmetric, the simulation can be executed in one 3D gap thus reducing the simulation time. The first step is the calculation of the effective cutting hob teeth (N) for which the simulation is executed, as illustrated in Fig. 3. The concept of the simulation is the creation of a 3D surface for each of the active teeth. This surface is developed by the rake edge's movement in the 3D space including all movements required in order to simulate the process. This surface defines the intrusion of the specific cutting tooth on the 3D gap. In the next simulation step, the workgear and the 3D surface are assembled and the volume of the gear is split by the surface, thus defining the

3D chip and gap. The final step of the simulation is the determination of the time course of the cutting force components, which is performed with the use of Kienzle–Victor's equations [14]. The results of the calculation include the cutting force components on every tooth of the hob as well as the total forces on the hob. The results are calculated on all three coordinate systems that are used by the program.

4 HOB3D Algorithm

As mentioned above, all the movements in HOB3D are transferred on the cutting edge. This means that the simulation setup includes a stationary gear and a hob rotating around it. In order to identify the cutting teeth, those are numbered. Tooth "0" is the tooth which has the local axis Y_1 parallel to local axis X_2 when it passes through the center of the gap. The tooth that passes after tooth "0" is named tooth "1" and the tooth previous to that is named tooth "-1," respectively. Due to the symmetry of the gear, the chip produced by a specific tooth is the same in all the gear gaps.

After the calculation of the penetration curve and the determination of the active teeth, the simulation begins with the mathematical description of the cutting tooth rake edge according to DIN 3972 [15]. This profile is converted into arcs and lines in the CAD environment in which HOB3D is embedded. The profile's sketch is then correctly positioned in the 3D space for every step of the simulation.

A 3D point must be identified in order to position the profile in the 3D space correctly. This point is the center of the hob at that specific moment. The center of the hob's movement forms a helix around the workgear. The helix radius is equal to $L_2 = d_h/2 + d_g/2 - t$, the helix pitch is equal to f_a and its axis is the Z axis of coordinate system (2). The axis of the hob is calculated after taking into account the setting angle from this 3D point. This axis is used in order to find the plane of the cutting edge at that simulation stage, in which a 2D sketch of the cutting edge is created. The coordinate system of the sketches has the axis of the hob as X and the axis that passes through the center of the hob as Y. The profile is positioned on the plane so that the distance between the center of the profile and the axis y is equal to n*e, where n is the number of the tooth studied and e is the axial pitch of the hob. Furthermore, the distance from the hob axis to the tip of the cutting tooth is equal to $d_h/2$. This process is repeated for a series of times increasing the rotational angle of the hob (phi) in every step. The result is a series of 3D placed profiles as presented on the third frame of the first line of Fig. 4. These profiles are combined resulting in a 3D surface that describes the movement of a specific tooth of the hob in the 3D space.

The 3D surface that was created is assembled with the 3D gap generated from the previous tooth. The positioning of the 3D surface on the assembly is accomplished by combining the two coordinate systems. The 3D surface path splits the volume of the workgear in two parts. The volume which is in the inner side of the surface is the nondeformed chip, and the other is the 3D gap after that pass.

After the end of the simulation, the output is the final geometry of the 3D gap, which corresponds to the space between two successive teeth of the gear, and all the nondeformed chips in every step of the process. These chips can be analyzed and data were obtained regarding the maximum chip thickness, chip cross-section area, and cutting forces.

The accuracy of the produced solid chip and gap geometry depends largely on the angular step, chosen for the hob rotation angle. It was found that the maximum error between the created and the theoretical surface increases as the angular step increases. For angular step of 2 deg this difference was smaller than 5×10^{-6} mm.

5 HOB3D Simulation Results

HOB3D is also equipped with a fully functional user friendly graphical user interface where the user can enter the simulation data, keep track of the simulation course, view and analyze the results. Several simulations of the manufacturing process of spur

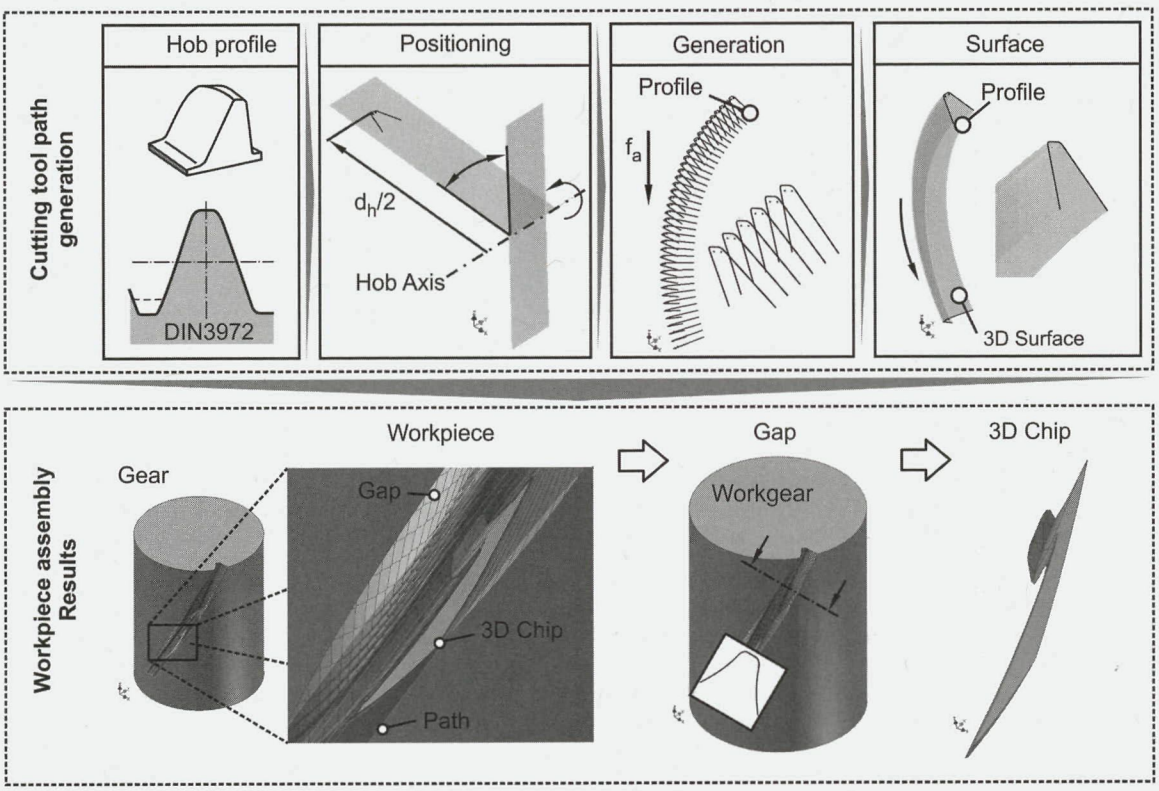

Fig. 4 HOB3D simulation process

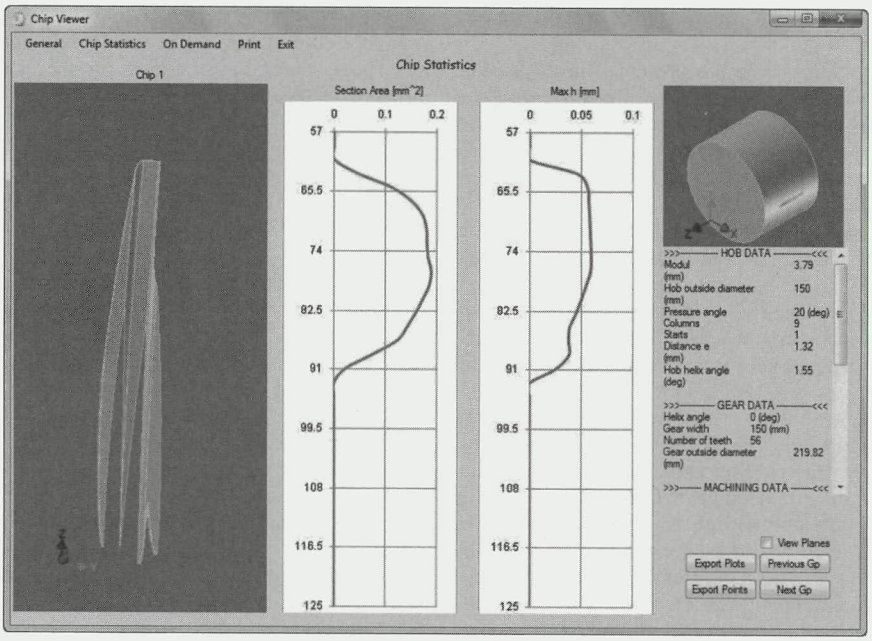

Fig. 5 Chip solid geometry characteristics

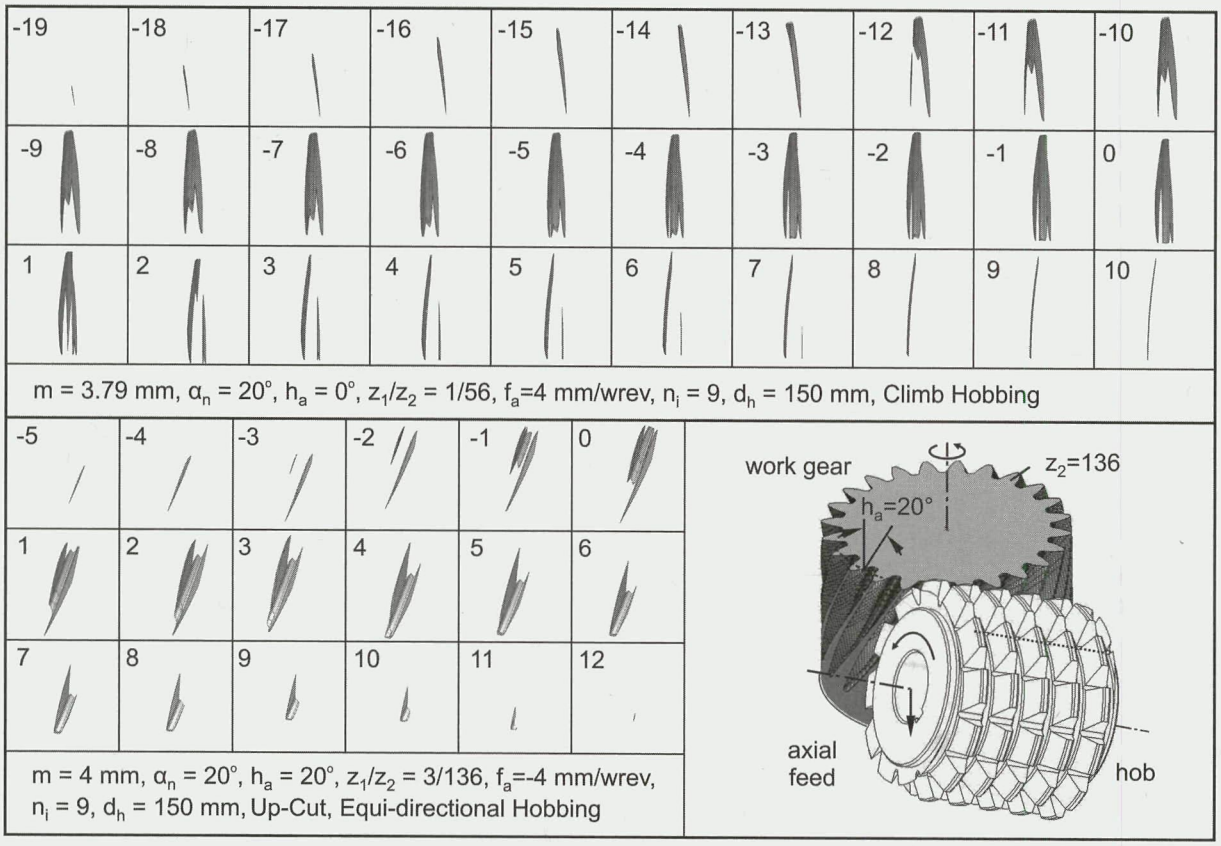

Fig. 6 HOB3D solid chip results

and helical gear were executed with the aid of this environment in order to verify the accuracy of the results. Figure 5 illustrates the solid chip geometry produced at the generating position (GP) = 1 on a spur gear. The cross-section area (A) and the maximum chip thickness (h_{max}) were calculated during the simulation and are presented in the form of 2D plots.

On the top section of Fig. 6, the chips that were produced during the simulation of the manufacturing of a spur gear are presented. As it can be observed, in order to form the final 3D gap, 30 teeth participate in the cutting process.

The process of cutting, as it can be observed from the 3D chips, begins with thin chips taken only from the leading flank. Next, the head of the cutter enters the machining process followed by the trailing flank. The cutting process continues in this manner until GP = 2 where the chip is divided and after a while the head of the cutter stops cutting. Eventually, the chips become thinner and

gradually the leading flank stops cutting followed by the trailing flank.

The solid chips for a helical case are presented in the bottom section of Fig. 6. The machining simulation of this case was executed with a three origin hob. As it can be easily noticed, the cuts required to produce the gap are considerably fewer than the ones in the spur case. In the case of the helical gear, there are 18 generating positions. The main reason for this fact is the increased number of origins which produces fewer and thicker chips. The process of cutting starts with the leading flank but it is followed immediately by the trailing flank, so the head starts to cut from the side of the trailing flank. The two volumes of the chip are unified in GP = 1. As the machining process continues, leading and trailing flanks stop cutting, leaving only the head of the cutter operating at the last GP.

The gap from the spur case was verified using the standard gap profiles introduced by Petri [11,12,16]. The process of the verification includes a section made parallel to the X_2Y_2 plane in order to acquire the 2D gap of the produced gear. The theoretical profile of the gear gap that is compared with the 2D gap consists of the root of the tooth, which is described by the profiles described by Petri and the involute curve. The measurement of the difference between theoretical and simulated profile showed that the model can accurately predict the topomorphy of the produced gear.

6 Calculation of Cutting Force Components With HOB3D

The prediction of the cutting force components is a crucial parameter in gear hobbing. HOB3D uses the equations of Kienzle–Victor so as to calculate the 3D components of the cutting forces based on the nondeformed chip geometry. In order to calculate the cutting forces, a series of cross-sections are made on the 3D chip on the plane of the cutting edge, see Fig. 7, where the outline of the chip is obtained for each one of them. The section is discritized as seen in detail A. The discritization is made with lines vertical to the cutting edge. For each elementary area, like the highlighted one in Fig. 7, the cutting force components must be calculated.

The first step of the calculation is the identification of the elementary chip of equivalent width and thickness, marked as b and h. The calculation is simple on the linear parts of the chip, whereas it becomes more complex on the head of the cutter, where the elementary chip takes an odd shape. This shape consists of one arc, two nonparallel lines, and one B-Spline and is simplified to a rectangular equivalent with the use of geometric equations and integrals. Next, the Kienzle–Victor's equations are implemented to produce the magnitude of the cutting force components on the cutting edge, using the material coefficients for the specific material as determined in the literature [17]. The force's point of application is in the middle of the elementary chip's side which belongs to the cutting edge. Three force components are calculated according to Kienzle–Victor F_r, F_s, and F_v. The first is parallel to the cutting edge, the second parallel to the cutting speed vector, and the last perpendicular to the prior two. The three force components are rotated in order to match the local coordinate system (1) and then added up in order to produce the total cutting forces on every cross-section. After all the sections are calculated, the total forces on the tooth are obtained, as presented on the bottom of Fig. 7. After the calculation of the cutting forces on the coordinate system (1), the cutting forces are rotated with the aid of transformation matrices and the cutting forces on systems (2) and (3) are calculated.

In Fig. 8, an example of the above described procedure is illustrated. The cross-sections made on the 3D chip that has been produced by the HOB3D are presented on the top right side of the figure, whereas the chip thickness on six of the cross-sections is illustrated on its left side. The cutting forces on coordinate system (1) are illustrated on the bottom line of the figure.

Figure 9 illustrates the total cutting forces of the spur gear case, as presented by the graphical user interface of HOB3D. The forces presented are calculated on coordinate system (2).

Results' accuracy depends greatly on the correct choice of the width of the elementary area. The error metrics used for the force calculation code was the difference between the chip cross-section area and the area of the equivalent rectangle. It was found that discritization with the width equal to the one-tenth of the profile arc has an error smaller than 0.7% of the measured area.

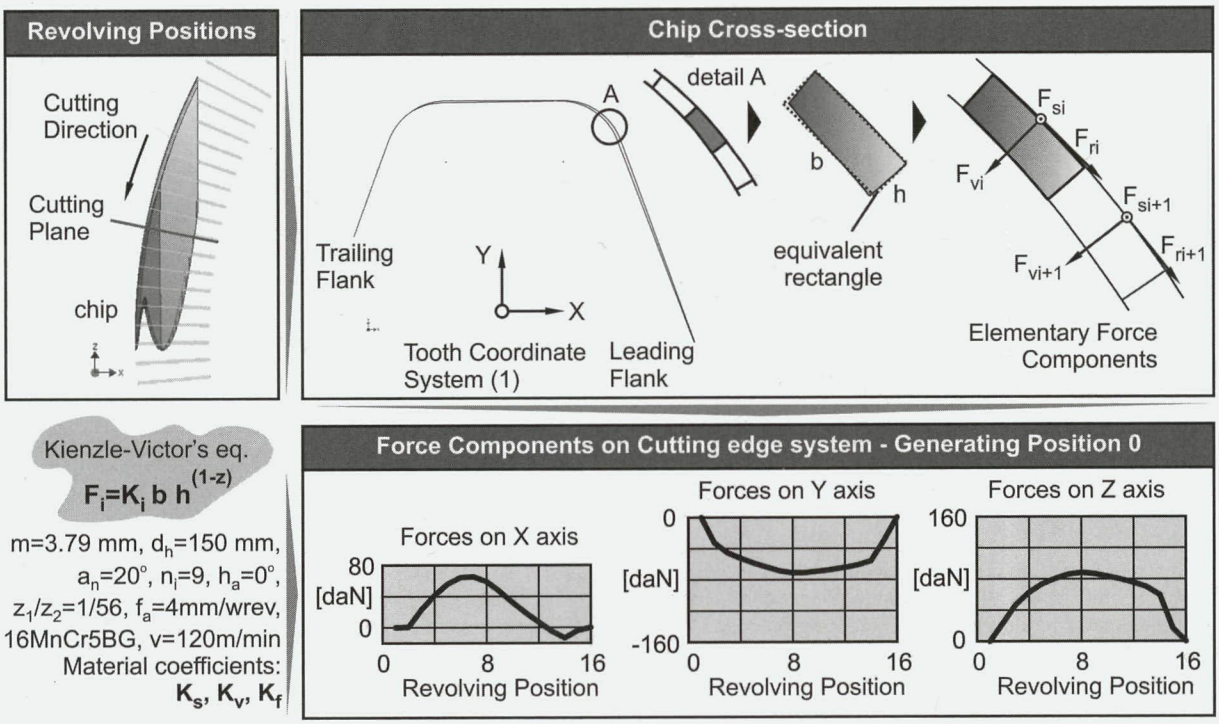

Fig. 7 Cutting force components calculation algorithm

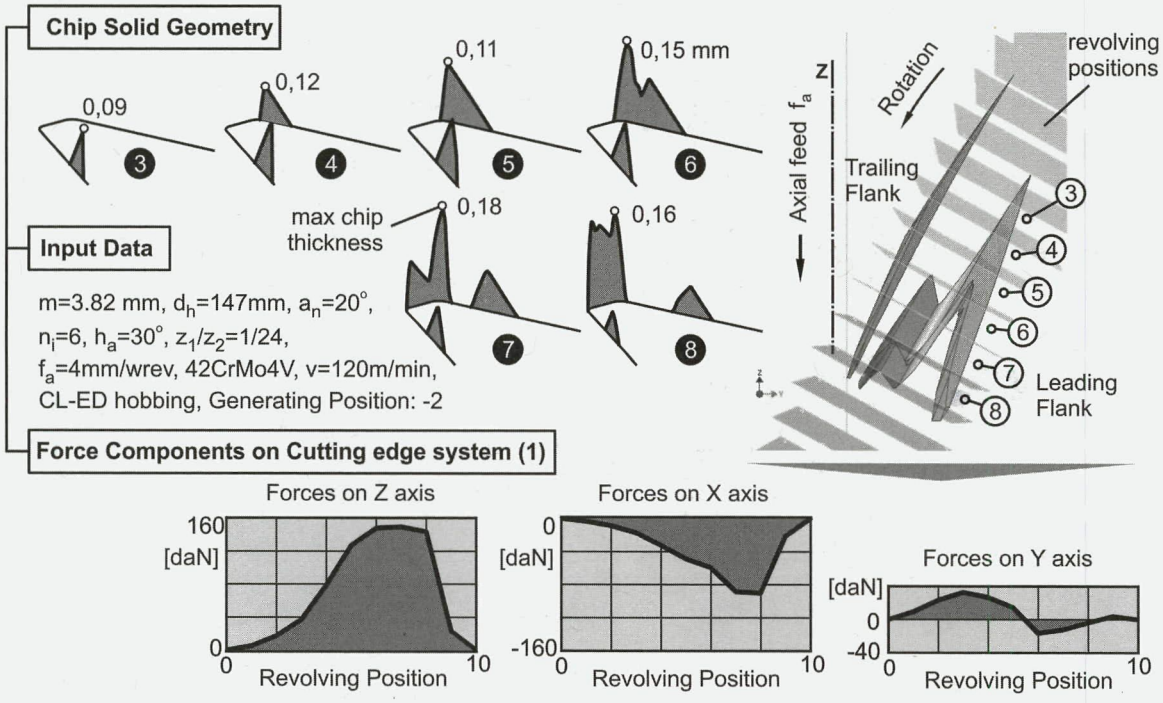

Fig. 8 Cutting force calculation in one generating position

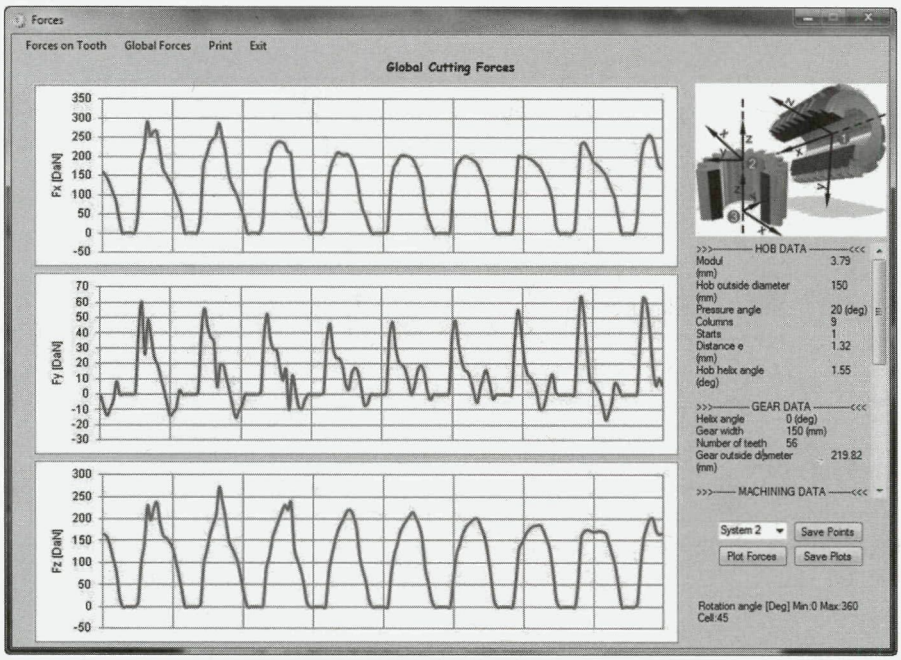

Fig. 9 HOB3D global cutting force viewer form

7 Cutting Force Components Verification

The verification of the force calculation module was conducted using experiments carried out by Bouzakis [2], who also used the tooth profile according to the reference profile II of Din-3972. The cases of climb and up-cut hobbing of a spur gear were examined and the cutting forces simulated on specific teeth were compared to the ones measured.

In Fig. 10, the results of the climb hobbing case are presented. As it can be seen, each column of the figure illustrates the measured and calculated cutting forces on one generating position. These cutting forces are measured on the coordinate system of the 3D gap (2). In most of the cases, the simulation code predicts not only the form but also the magnitude of the cutting forces. Especially in generating positions – 6 and 2, the simulation results are almost identical to the ones measured.

Figure 11 illustrates the simulated and measured cutting force components in four generating positions in the case of up-cut hobbing. The simulation results of this case confirm the validity of the calculation code, predicting the developed cutting force components in all three axes accurately.

In both cases, the simulated values of the cutting process are very close to the real ones. Minor differences between them, especially in the Y axis of the climb hobbing case, occur due to the

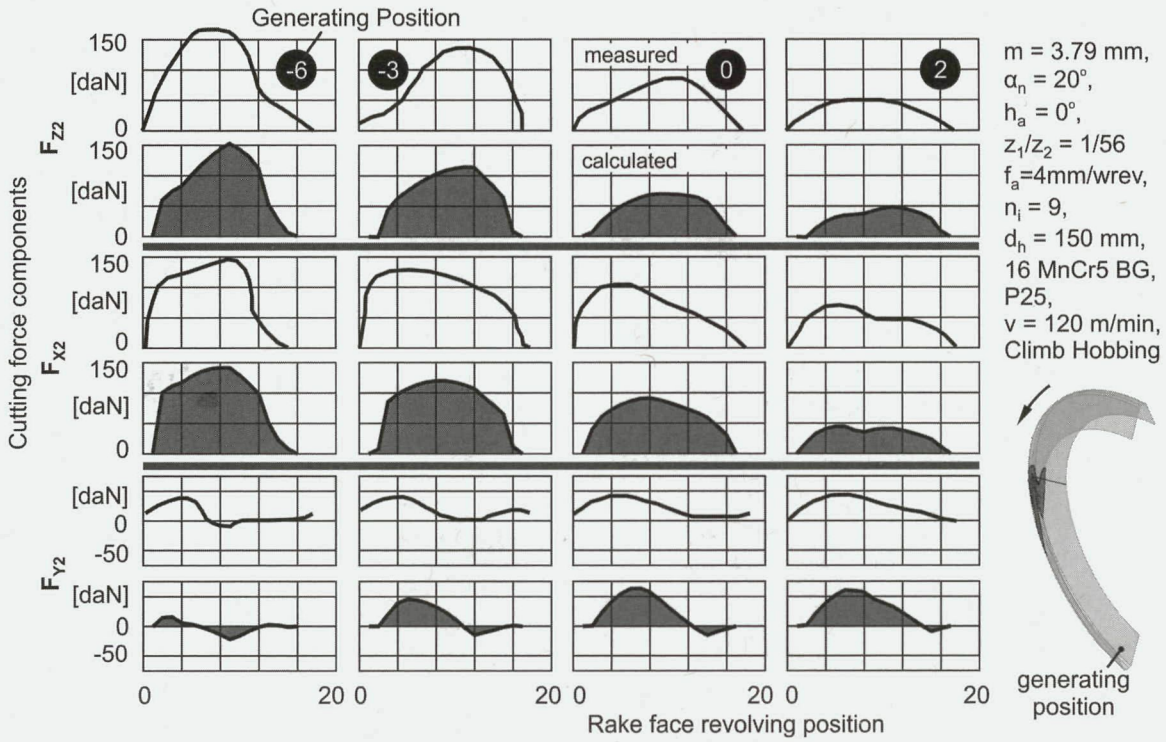

Fig. 10 Comparison between calculated and measured cutting forces in climb hobbing

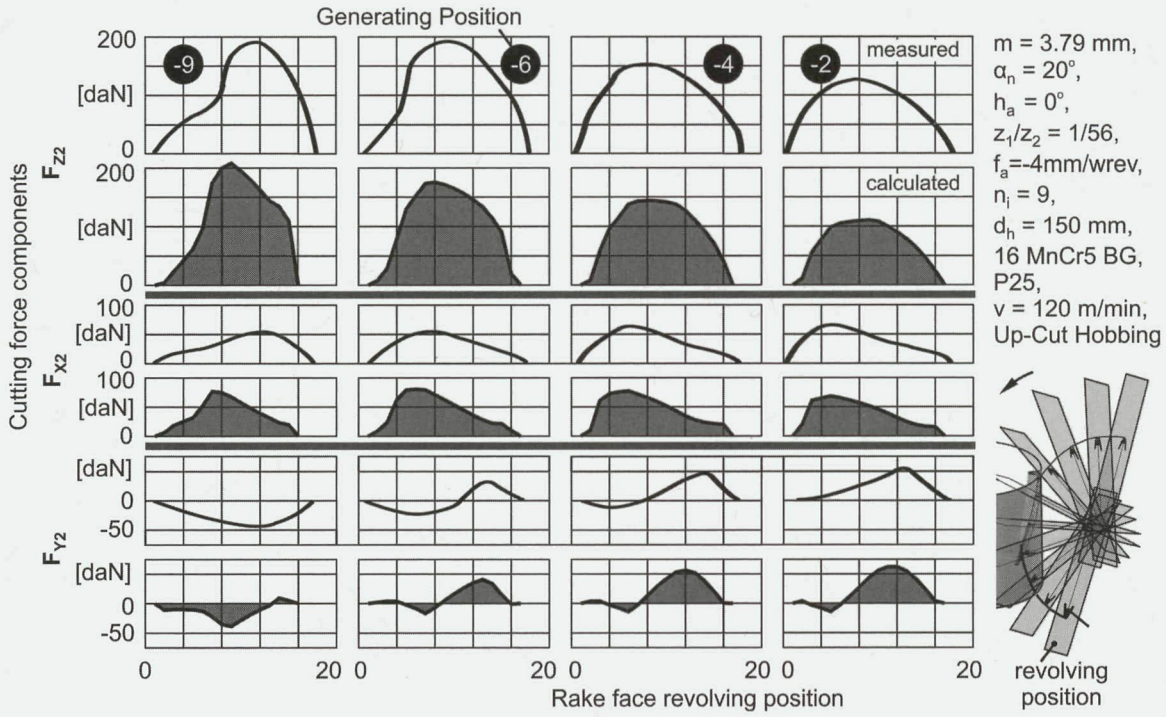

Fig. 11 Comparison between calculated and measured cutting forces in up-cut hobbing

fact that the chips created by different flanks of the gear collide inside the gap of the gear, creating extra cutting forces or reducing them due to the cross-cancellation of cutting forces.

8 Conclusion

A novel simulation code for the manufacturing process of gear hobbing was presented in this paper. The simulation code, called HOB3D, was embedded on a commercial CAD environment and can simulate the cutting process accurately. The resulting gap was successfully verified using analytical equations. The cutting force components were determined based on the undeformed chip as calculated by HOB3D. The cutting forces were also verified through experiments.

Acknowlegment

This research has been cofinanced by the European Union (European Social Fund—ESF) and Greek national funds through the

Operational Program "Education and Lifelong Learning" of the National Strategic Reference Framework (NSRF)—Research Funding Program: Heracleitus II. Investing in knowledge society through the European Social Fund.

Nomenclature

GP = generating position
RP = revolving position
CL = climb hobbing
UC = up-cut hobbing
ED = equidirectional hobbing
CD = counterdirectional hobbing
FEM = finite elements method
γ = hob helix angle (deg)
ε = hob axial pitch (mm)
f_a = axial feed (mm/rev)
t = cutting depth (mm)
v = cutting speed (m/min)
m = workgear and hob tool module (mm)
n_i = number of hob columns
z_1 = number of hob origins
z_2 = number of workgear teeth
d_g = external workgear diameter (mm)
d_h = external hob diameter (mm)
h_a = gear helix angle (deg)

Reference

[1] Sulzer, G., 1974, "Leistungssteigerung bei der Zylinderradherstellung durch genaue Erfassung der Zerspankinematik," Ph.D. Dissertation, Rheinisch-Westfaelische Technische Hochschule, Aachen, Germany.
[2] Bouzakis, K. D., 1980, "Konzept und technologishe Grundlagen zur automatisierten Erstellung optimaler Bearbeitungsdaten beim Waelzfraese," Habilitation, Rheinisch-Westfaelische Technische Hochschule, Aachen, Germany.
[3] Gutman, P., 1988, "Zerspankraftberechnung beim Waelzfraesen," Ph.D. Dissertation, Rheinisch-Westfaelische Technische Hochschule, Aachen, Germany.
[4] Tondorf, J., 1978, "Erhoehung der Fertigungsgenauigkeit beim Waelzfraesen durch systematische Vermeidung von Aufbauschneiden," Ph.D. Dissertation, Rheinisch-Westfaelische Technische Hochschule, Aachen, Germany.
[5] Venohr, G., 1985, "Beitrag zum Einsatz von hartmetall Werkzeugen beim Waelzfraesen," Ph.D. Dissertation, Rheinisch-Westfaelische Technische Hochschule, Aachen, Germany.
[6] Antoniadis, A., 1989, "Determination of the Impact Tool Stresses During Gear Hobbing and Determination of Cutting Forces During Hobbing of Hardened Gears," Ph.D. Dissertation, Aristoteles University of Thessaloniki, Greece.
[7] Antoniadis, A., Vidakis, N., and Bilalis, N., 2002, "Fatigue Fracture Investigation of Cemented Carbide Tools Used in Gear Hobbing, Part I: FEM Modeling of Fly Hobbing and Computational Interpretation of Experimental Results," ASME J. Manuf. Sci. Eng., 124(4), pp. 784–791.
[8] Antoniadis, A., Vidakis, N., and Bilalis, N., 2002, "Fatigue Fracture Investigation of Cemented Carbide Tools Used in Gear Hobbing, Part II: The Effect of Cutting Parameters on the Level of Tool Stresses—A Quantitive Parametric Analysis," ASME J. Manuf. Sci. Eng., 124(4), pp. 792–798.
[9] Bouzakis, K., Kompogiannis, S., Antoniadis, A., and Vidakis, N., 2002, "Gear Hobbing Cutting Process Simulation and Tool Wear Prediction Models," ASME J. Manuf. Sci. Eng., 124(1), pp. 42–51.
[10] Friderikos, O., 2008, "Simulation of Chip Formation and Flow in Gear Hobbing Using the Finite Element Method," Ph.D. thesis, Aristoteles University of Thessaloniki, Greece.
[11] Dimitriou, V., Vidakis, N., and Antoniadis, A., 2007, "Advanced Computer Aided Design Simulation of Gear Hobbing by Means of 3-Dimensional Kinematics Modeling," ASME J. Manuf. Sci. Eng., **129**, pp. 911–918.
[12] Dimitriou, V., and Antoniadis, A., 2008, "CAD-Based Simulation of the Hobbing Process for the Manufacturing of Spur and Helical Gears," Int. J. Adv. Manuf. Technol., **41**(3–4), pp. 347–357.
[13] Michalski, J., and Skoczylas, L., 2008, "Modelling the Tooth Flanks of Hobbed Gears in the CAD Environment," Int. J. Adv. Manuf. Technol., **36**(7), pp. 746–751.
[14] Kienzle, O., and Victor, H., 1957, "Spezifische Shnittkraefte bei der Metallbearbeitung," Werkstattstehnik und Maschinenbau, Bd. 47, H.5.
[15] DIN 3972, 1981, *Bezugsprofile von Verzahnwerkzeugen fuer Evolventenverzahnungen Nach DIN 867*, Taschenbuch 106, Beuth Verlag, Berlin.
[16] Petri, H., 1975, "Zahnhuß—Analyse bei außenverzahnten Evolventenstirnraedern: Teil III Berechnung," Antriebstechnik, **14**(5), pp. 289–297.
[17] König, W., and Essel, K., 1973, *Spezifische Schnittkraftwerte für die Zerspanung metallischer Werkstoffe*, Verlag Stahleisen, Düsseldorf.